JOC The Journal of Organic Chemistry

Article

pubs.acs.org/joc

Correlations between Computation and Experimental Thermodynamics of Halogen Bonding

Michael G. Chudzinski and Mark S. Taylor*

Department of Chemistry, University of Toronto, 80 St. George Street, Toronto, Ontario M5S 3H6, Canada

Supporting Information

ABSTRACT: Correlations between experimental, solution-phase thermodynamic data and calculated gas-phase energies of interaction are investigated for noncovalent halogen bonding interactions between electron-deficient iodo compounds and Lewis bases. The experimental data consist of free energies of interaction spanning roughly 7 kcal/mol; they encompass halogen bonds involving both organic (iodoperfluoroarene or iodoperfluoroalkane) and inorganic (I_2, IBr, ICN) donors with nitrogen- and oxygen-based acceptors and are divided into two sets according to the identity of the solvent in which they were determined (alkanes or CCl_4). Adiabatic energies of halogen bonding were calculated using a variety of methods, including 22 DFT exchange-correlation functionals, using geometries optimized at the MP2/6-31+G(d,p) level of theory. Certain DFT functionals, particularly the B97-1, B97-2, and B98 family, provide outstanding linear correlations with the experimental thermodynamic data, as assessed by a variety of statistical methods.

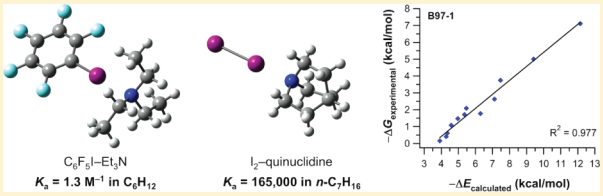

INTRODUCTION

Halogen bonds are attractive noncovalent interactions between covalently bound, electron-deficient halogen atoms and Lewis bases.[1] Although numerous examples of halogen bonding (XB) have been studied over the past century,[2] it is only in the past 10−15 years that the generality and utility of this interaction have come into focus. Current research on XB encompasses applications in condensed phases[3] (materials chemistry and crystal engineering) and in solution-phase molecular recognition,[4] as well as studies of its roles in biomolecular conformation and drug design (Figure 1).[5]

In parallel with these studies, there has been much effort devoted to elucidating the nature of the XB interaction. Early attempts to understand XB formulated it as a charge-transfer interaction as defined by Mulliken:[6] for interactions of molecular iodine with a variety of Lewis bases (the first halogen bonds for which solution-phase thermodynamic data were obtained[2a]), the UV−vis absorption spectroscopic changes upon complexation are consistent with this hypothesis. In recent years, the "σ-hole" hypothesis has been proposed, invoking an electrostatic interaction of the Lewis base with the site of partial positive electrostatic potential at the halogen (the σ-hole: Figure 1).[7] Several computational studies[8] suggest that the extent of electrostatic versus charge-transfer character of the XB interaction is dependent on the identity of the halogen-bond donating group. Weaker halogen bonds, as exemplified primarily by those of organic donors, are thought to be more electrostatic in nature. This is in contrast to stronger halogen bonds formed by inorganic donors, for which greater covalent or charge-transfer character is invoked. In particular, Zou and co-workers[8b] demonstrated that different linear trends between organic and inorganic donors arise upon examining the calculated interaction energy as a function of charge-transfer or electrostatic character. Both the charge-transfer and electrostatic hypotheses are consistent with the observed directionality of XB, in which a 180° R−X···B angle

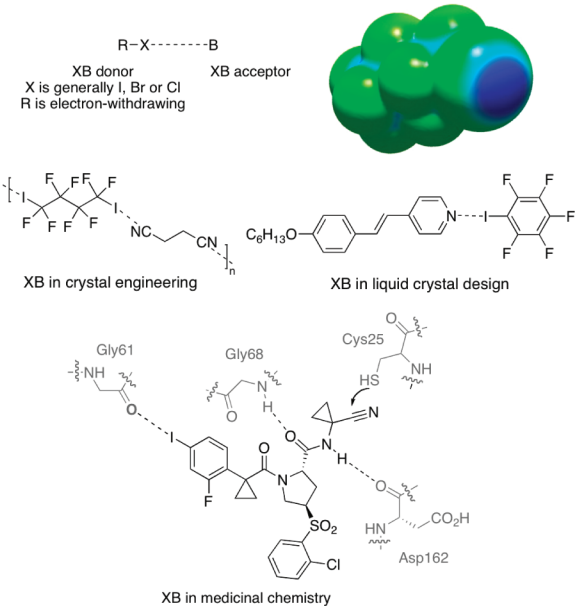

Figure 1. Halogen bonding interaction, calculated (MP2/6-31+G-(d,p)-LANL2DZdp) molecular electrostatic potential surface for C_4F_9I (blue color indicates regions of partial positive charge), and representative applications of halogen bonding in condensed phases (from ref 3) and medicinal chemistry (from ref 5b).

Received: February 7, 2012
Published: March 20, 2012

   dx.doi.org/10.1021/jo300279m | J. Org. Chem. 2012, 77, 3483−3491

is strongly preferred. Theoretical studies[8a,9] indicate that contributions from dispersion and polarization are also relevant to the nature of the XB interaction, particularly for weaker interactions where the directional preferences are more relaxed. The variation of the nature of the interaction as a function of the partners involved is a rather unique aspect of XB, and one that presents a challenge from the standpoint of computational modeling. To elucidate these issues, and to evaluate the ability of theoretical methods to correctly describe the geometrical and thermodynamic properties of halogen-bonded complexes, computational studies of XB have been undertaken by several research groups.[8−10]

Of the many publications describing computational modeling of XB, few involve comparisons between calculated and experimental thermodynamic data. Relationships of this type with solution-phase binding data are useful in a wide variety of settings and have been explored in considerable detail for the hydrogen bonding (HB) interaction.[11] An overwhelming proportion of computational studies on XB have correlated calculated data with gas-phase geometries,[12] experimentally determined electron densities,[13] changes in NMR chemical shift,[14] or other high-level calculations[9] rather than solution-phase binding data. A few recent reports have evaluated experimental thermodynamic data in the context of individual or structurally related (families of) halogen bond donors. Laurence and coworkers[15] compiled a large data set of XB association constants (K_a) between iodine (I_2) and structurally diverse acceptors in order to construct a Lewis basicity scale. They found that the I_2 basicity scale could be employed in linear free energy relationships with the strengths of halogen bonds involving other inorganic donors (ICl, IBr, Br_2). However, this scale could only be applied to organic donors (e.g., C_6F_5I, ICN) after incorporating an additional electrostatic parameter (experimental hydrogen bond basicity (pK_{BHX}) or computed electrostatic potential ($V_{s,min}$)) to the linear regression. These results represent experimental support for the proposal that the relative contributions of charge-transfer and electrostatic components differ between organic and inorganic donors. Other studies have taken advantage of recently obtained thermodynamic data for organic halogen bond donors, particularly iodoperfluoroalkanes and/or arenes: modest levels of correlation with the experimental data have been obtained using Hunter's pairwise electrostatic model,[16] electrostatic potential surfaces,[17] or energies of interaction calculated with a limited set of methods (density functional theory with the B3LYP hybrid functional).[18]

The goal of the present study is to investigate correlations between experimentally determined free energies of XB and calculated energies of interaction for a diverse range of donor−acceptor pairs. The experimental data set used for this purpose encompasses both inorganic and organic halogen bond donors, as well as nitrogen- and oxygen-based acceptors, and the association constants (determined in noncompetitive solvent) span more than 5 log units. Although it is relatively limited in size when compared to those generally used to evaluate the performance of noncovalent interactions in benchmarking studies,[19] it comprises XB interactions that vary widely in structure and thermodynamics and presents an opportunity to systematically evaluate a wide range of computational methods in a manner that has not previously been reported. Of particular interest to us was the prospect of identifying relatively low-cost, generally accessible computational techniques able to accurately model the thermodynamics of halogen bonding; such techniques would be useful for probing noncovalent Lewis base/halogen interactions relevant to catalysis,[20] molecular recognition,[4] and medicinal chemistry.[5b] Our results reveal that the B97-1, B98, and B97-2 DFT functionals display excellent levels of correlation with this diverse set of experimental data, outperforming other commonly applied DFT functionals as well as the well-established MP2 *ab initio* method.

COMPUTATIONAL METHODOLOGY

Experimental Halogen Bonding Data. The experimental XB data set consists of the 12 pairwise free energies of interaction between three iodinated donors (iodine (I_2), iodoperfluorobenzene (C_6F_5I), and 1-iodoperfluorooctane ($C_8F_{17}I$)) and four Lewis bases (triethylamine (Et_3N), di-*n*-butyl sulfoxide (Bu_2SO), tri-*n*-butylphosphine oxide (Bu_3PO), and quinuclidine; Figure 2 and Table 1). The association constants (K_a)

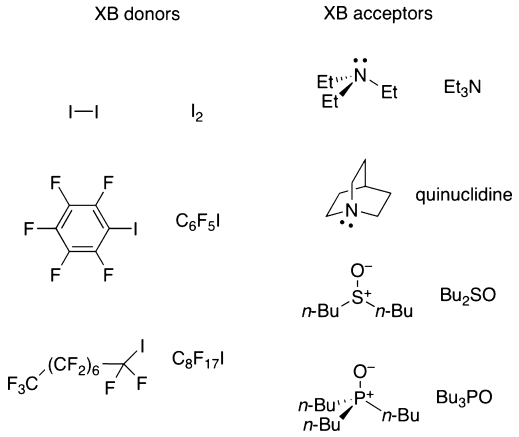

Figure 2. Structures of the XB donors and acceptors listed in Table 1.

Table 1. Association Constants (K_a) and Free Energies of Interaction (ΔG_{exptl}) for Halogen-Bonded Complexes in Alkane Solvent

complex	K_a[a] (M^{-1})	ΔG_{exptl}[b] (kcal/mol)
C_6F_5I−Et_3N[c]	1.3 ± 0.2	−0.2 ± 0.1
C_6F_5I−Bu_2SO[c]	2.0 ± 0.4	−0.4 ± 0.1
$C_8F_{17}I$−Et_3N[c]	2.8 ± 0.6	−0.6 ± 0.1
$C_8F_{17}I$−Bu_2SO[c]	6.2 ± 1.2	−1.1 ± 0.1
C_6F_5I−Bu_3PO[c]	12 ± 2.5	−1.5 ± 0.1
$C_8F_{17}I$−Bu_3PO[c]	18 ± 4	−1.7 ± 0.1
C_6F_5I−quinuclidine[c]	20 ± 4	−1.8 ± 0.1
$C_8F_{17}I$−quinuclidine[c]	34 ± 7	−2.1 ± 0.1
I_2−Bu_2SO[d]	85 ± 17	−2.6 ± 0.1
I_2−Bu_3PO[d]	560 ± 110	−3.7 ± 0.1
I_2−Et_3N[d,e]	4690 ± 940	−5.0 ± 0.1
I_2−quinuclidine[d,e]	165000 ± 33000	−7.1 ± 0.1

[a]Association constant (K_a) for the halogen-bonding interaction in cyclohexane solvent, determined by fitting changes in ^{19}F NMR chemical shift or charge-transfer band as a function of Lewis base concentration to a 1:1 binding isotherm. [b]Free energy of interaction calculated from K_a. [c]Data from ref 18a. [d]Data from ref 15. [e]Association constants were determined in heptane.

from which these free energies were calculated were determined by ^{19}F NMR[18a] or UV−vis[15] titrations in cyclohexane or heptane solvent at 298 K. Data in alkane solvent were chosen so as to minimize effects related to solvent polarity or competitive solvation, enabling comparisons with gas-phase

dx.doi.org/10.1021/jo300279m | J. Org. Chem. 2012, 77, 3483−3491

calculations. The free energies of interaction range from 0.2 to 7.1 kcal/mol, and differences in the behavior of the organic and inorganic donors are evident: for example, the order of binding of the four Lewis bases with the iodoperfluorocarbons is quinuclidine > Bu_3PO > Bu_2SO > Et_3N, but with I_2 it is quinuclidine > Et_3N > Bu_3PO > Bu_2SO. Such deviations in basicity as a function of the halogen bond donor may reflect differing charge transfer contributions (see below) and likely underlie the challenges in correlating data obtained for organic donors with those for I_2 interactions.

Computational Methods. Quantum chemical calculations were carried out with the Gaussian 09[21] suite of programs. To expedite the calculations, simplified models of the compounds listed in Table 1 were employed: 1-iodofluorobutane (C_4F_9I) in place of $C_8F_{17}I$, dimethyl sulfoxide (Me_2SO) in place of Bu_2SO, and trimethylphosphine oxide (Me_3PO) in place of Bu_3PO. Geometry optimizations were performed in the gas phase using the MP2[22] *ab initio* method, employing the double-ζ 6-31+G(d,p) Pople basis sets[23] for all atoms except bromine and iodine, for which the double-ζ LANL2DZ basis set and effective core potential (ECP) were used,[24] augmented by polarization functions of d symmetry and diffuse functions of p symmetry;[25] this basis set is abbreviated LANL2DZdp in this paper. The LANL2DZdp basis set was downloaded from the EMSL Basis Set Exchange.[26] Geometry optimizations were carried out without constraints, using the default convergence criteria for the Gaussian software, except in cases that required tighter convergence criteria to obtain true minima (as indicated by the absence of imaginary frequencies).[27] Vibrational frequency calculations were carried out at the same level of theory as the geometry optimizations and indicated that the stationary points were minima, lacking imaginary frequencies. For all calculations, tight SCF convergence criteria and the default grid size (FineGrid: 75 radial shells; 302 angular points) were employed. The basis set superposition error (BSSE) for noncovalent complexes was estimated using the counterpoise method of Boys and Bernardi.[28]

The energies of interaction were estimated by subtracting the sum of the calculated electronic energies of the isolated partners from the electronic energy of the noncovalent complex, according to eq 1.

$$\Delta E_{\text{calculated}} = E_{\text{complex}} - [E_{\text{donor}} + E_{\text{acceptor}}] \quad (1)$$

The obtained electronic energies of interaction were corrected for scaled (0.9657)[29] zero-point energy differences (obtained from the frequency calculations described above) and for basis set superposition errors (see above).

Several exchange-correlation functionals were evaluated in the context of density functional calculations: B3LYP (Becke's three-parameter hybrid method[30] using the correlation functional of Lee, Yang and Parr[31]); M05,[32] M05-2X,[33] M06,[34] M06-2X,[34] M06-HF,[35] and M06-L[36] (hybrid meta and local meta functionals developed by Truhlar and co-workers); ωB97,[37] ωB97X,[37] ωB97X-D[38] (long-range corrected functionals developed by Head-Gordon and co-workers); X3LYP (using the exchange functional developed by Goddard III[39] along with the LYP correlation functional); PBE1PBE[40] (also termed PBE0 in the literature); HCTH/407[41] (abbreviated HCTH in this paper); B97-1;[42] B97-2;[43] B98;[44] B97-D[45] (Grimme's variation of B97 with dispersion included); B2PLYP,[46] B2PLYP-D,[47] MPW2PLYP,[48] MPW2PLYP-D[47] (Grimme's double hybrid functionals, both excluding and including dispersion, respectively). The functionals chosen for evaluation were developed to model hydrogen bonding, charge transfer, dipole, dispersion or noncovalent interactions accurately and/or have been demonstrated to model these interactions well.[33,49]

RESULTS AND DISCUSSION

Calculated Gas-Phase Halogen Bonding Geometries. Key features of the MP2-calculated gas-phase geometries for the 12 halogen-bonded complexes are summarized in Table 2.

Table 2. Halogen Bond Distances ($D_{I\cdots X}$) and Angles ($\angle_{Y-I\cdots X}$) of Complexes Optimized at the MP2/6-31+G(d,p)-LANL2DZdp Level of Theory

complex	$D_{I\cdots X}$ (Å)	$\angle_{Y-I\cdots X}$ (deg)	$D_{I\cdots X}$ (Å)/$\sum$(vdW)[a]
C_6F_5I–Et_3N	2.82	179.8	0.80
C_6F_5I–DMSO	2.80	178.6	0.80
C_4F_9I–Et_3N	2.81	178.3	0.80
C_4F_9I–DMSO	2.79	177.9	0.80
C_6F_5I–Me_3PO	2.79	177.3	0.80
C_4F_9I–Me_3PO	2.78	177.5	0.79
C_6F_5I–quinuclidine	2.70	179.9	0.76
C_4F_9I–quinuclidine	2.69	178.4	0.76
I_2–DMSO	2.62	179.6	0.75
I_2–Me_3PO	2.62	178.8	0.75
I_2–Et_3N	2.55	180.0	0.72
I_2–quinuclidine	2.48	180.0	0.70

[a]The calculated XB distance divided by the sum of the van der Waals radii of the individual atoms. Radii from ref 50.

For each complex, the noncovalent bond angles $\angle_{Y-I\cdots X}$ are near-linear and the halogen-bond distances $D_{I\cdots X}$ are significantly shorter than the sum of van der Waals radii, in agreement with previous experimental and computational studies. Figure 3 depicts an inverse relationship between the experimental free energies of interaction ($-\Delta G_{exptl}$) from Table 1 and the MP2 calculated gas-phase X···B bonding distances for the model complexes shown in Table 2. Similar relationships between calculated interaction energies and bond distances have been documented previously.

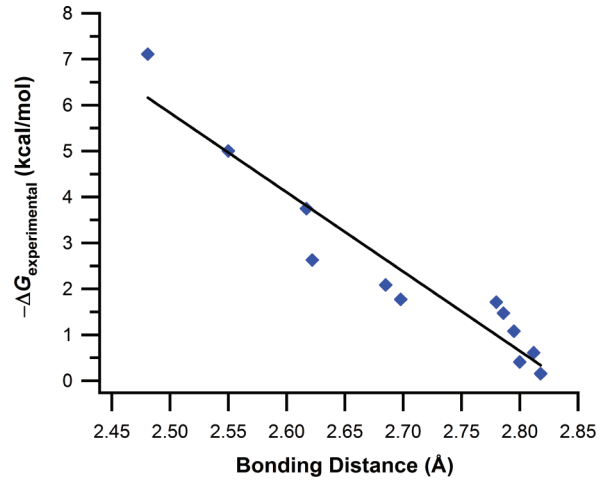

Figure 3. Plot of experimental free energy of binding ($-\Delta G_{exptl}$ from Table 1) versus calculated bonding distance for the corresponding model complex (from Table 2).

Correlations between Experimental Thermodynamic Data and Hunter's Pairwise Electrostatic Interaction Model. The pairwise electrostatic interaction model developed

dx.doi.org/10.1021/jo300279m | J. Org. Chem. 2012, 77, 3483–3491

by Hunter was used to probe the assertion that the relative contributions of electrostatic and charge-transfer components differ between organic and inorganic halogen bond donors. According to the Hunter model, solution-phase free energies of interaction between a donor and acceptor can be approximated by eq 2, which takes into account electrostatic donor−acceptor, donor−solvent, acceptor−solvent, and solvent−solvent interactions as well as an unfavorable entropy of association (the latter is assumed to be constant).[51]

$$\Delta G = -(\alpha - \alpha_S)(\beta - \beta_S) + 6\ \text{kJ/mol} \quad (2)$$

The donor (α) and acceptor abilities (β) of the interaction partners and those of the solvent (α_S and β_S) are based on experimental hydrogen bonding data or on semiempirical (AM1) molecular electrostatic potential calculations. This model has proved to be broadly applicable to the study of noncovalent interactions in solution; in particular, excellent levels of quantitative agreement have been obtained with experimental hydrogen bonding association constants spanning more than 5 orders of magnitude.[52]

Figure 4 indicates that there is a poor level of correlation between the experimental free energies of interaction from Table 1

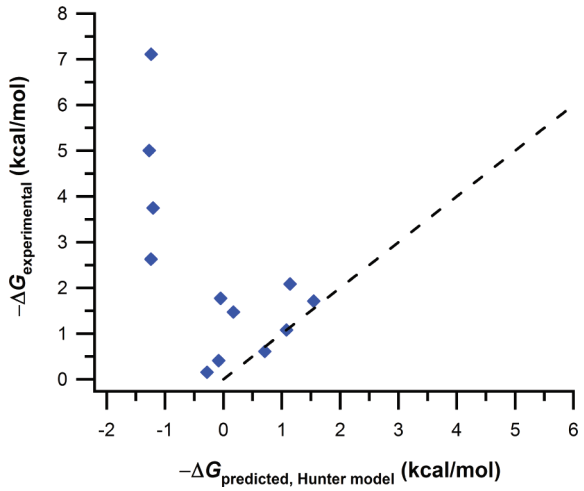

Figure 4. Plot of experimental free energies of halogen bonding in alkane solvent versus those predicted by Hunter's pairwise electrostatic model.

and those predicted by the electrostatic model described in the preceding paragraph. The donor abilities of C_6F_5I (α = 2.5), $C_8F_{17}I$ (α = 1.9), and I_2 (α = 1.3) were estimated using AM1 molecular electrostatic potential calculations for consistency with Hunter's approach, and values of α_S and β_S for alkane solvents were obtained from a recent publication.[53] The interactions of I_2 (represented by the four data points grouped on the left side of the graph) pose the most significant problem: whereas electrostatic potential calculations suggest that I_2 should be the weakest of the three donors, it in fact is the strongest, by a considerable margin.[54] The organic donors comprise a separate cluster of data, closer to the line $y = x$, as noted previously by our group[18a] and that of Hunter.[16] As described above, the relative acceptor abilities of the four Lewis bases differ depending on the identity of the halogen bond donor (organic donors versus I_2; Table 1). These results, along with the linear free-energy relationships explored previously by Laurence (see above),[15] are consistent with the hypothesis that there is a greater charge-transfer contribution to the interactions of I_2 relative to those of the iodoperfluorocarbon donors.

Correlations between Calculated Gas-Phase Adiabatic Energies of Interaction and Experimental Free Energies of Halogen Bonding in Alkane Solvent. The geometries from MP2 optimizations were employed as the basis for single-point energy calculations as described in the previous section (Hartree−Fock or density functional theory, with the 21 listed exchange-correlation functionals), with the aim of examining correlations between the calculated gas-phase adiabatic energies of interaction and solution-phase free energies of XB. Agreement between computation and experiment in terms of absolute values was not expected; the calculated energies of interaction are distinct from free energies, and solvent effects are generally not negligible, even in relatively inert media such as alkanes. However, linear correlations between the data sets could be possible, provided that the magnitudes of the desolvation and entropy terms (among others) are roughly constant across the series of complexes studied. In regard to the entropy term, the assumption of a constant, unfavorable ΔS for 1:1 interactions involving a single donor and acceptor site on the respective partners underlies the Hunter model (see above), which has been applied to diverse hydrogen bonding interactions in media ranging from alkanes to DMSO. To the extent that the primary solvent−solute interactions in alkane medium are dispersion-driven, and given that each of the associations in Table 1 involves a nitrogen or oxygen-based lone pair interacting with an iodine atom (thus engaging roughly similar amounts of accessible surface area in each case), the assumption of similar desolvation terms may not be completely unreasonable. In any event, relationships between the experimental data in alkane solvent and the gas-phase calculated data for the model complexes were indeed observed. Table 3 lists the calculated energies of interaction and basis set superposition errors for the top six performing DFT functionals, along with the commonly employed MP2 method and B3LYP functional, while Figures 5 and 6 show plots of solution-phase experimental ($-\Delta G_{exptl}$, from Table 1) versus gas-phase calculated ($-\Delta E_{calcd}$, from Table 3) energies of interaction for the same set of data. Full data sets are provided in the Supporting Information. Significant levels of correlation between $-\Delta G_{exptl}$ and $-\Delta E_{calcd}$ were observed for the MP2 (R^2 = 0.89) and B3LYP (R^2 = 0.88) methods, and certain DFT functionals (B97-1, B98, B97-2, PBE1PBE, and ωB97X) provided superior performance ($R^2 > 0.95$).

Table 4 summarizes the results of a detailed analysis of correlations between experiment and computation for all methods assessed here, ranked in descending order in terms of performance. Each model, as determined by linear regression of calculated energies and experimental energies of interaction, was subjected to cross-validation using the leave-one-out (LOO) method. The results indicate that the B97-1 functional offers superior performance in modeling the XB interaction across this diverse data set, with an R^2 value of 0.98 and root-mean-square error (RMSE) of 0.30 kcal/mol. A similar conclusion is reached by analysis of the cross-validated coefficient of determination, which offers a measure of the predictability of a model (Q^2 = 0.97 for the B97-1 model). Excellent correlations and predictability were also observed for the related B98 and B97-2 functionals as well as the PBE1PBE functional ($R^2 > 0.95$, $Q^2 > 0.94$).

That certain DFT functionals outperform B3LYP in correlations with thermodynamics of XB is not surprising, given the results of previous benchmarking studies of DFT functionals in

dx.doi.org/10.1021/jo300279m | J. Org. Chem. 2012, 77, 3483−3491

Table 3. Calculated Gas-Phase Energies of Interaction (ΔE) (kcal/mol) and Basis Set Superposition Errors (BSSE) (kcal/mol) for Halogen-Bonded Complexes Calculated with Various Methods[a]

	MP2		B3LYP		B97-1		B98	
complex	ΔE	BSSE	ΔE	BSSE	ΔE	BSSE	ΔE	BSSE
C_6F_5I–Et_3N	−0.119	3.94	0.0123	0.74	−3.91	0.76	−2.94	0.76
C_6F_5I–DMSO	−1.22	2.14	−2.09	0.44	−4.29	0.46	−3.77	0.46
C_4F_9I–Et_3N	−0.340	3.68	−0.599	0.64	−4.36	0.66	−3.41	0.66
C_4F_9I–DMSO	−1.38	2.06	−2.51	0.41	−4.59	0.42	−4.09	0.42
C_6F_5I–Me_3PO	−1.72	2.15	−2.73	0.44	−4.97	0.46	−4.44	0.46
C_4F_9I–Me_3PO	−1.99	2.06	−3.26	0.42	−5.36	0.43	−4.86	0.44
C_6F_5I–quinuclidine	−1.38	3.70	−2.91	0.70	−6.29	0.71	−5.48	0.70
C_4F_9I–quinuclidine	−0.468	3.42	−2.16	0.62	−5.47	0.62	−4.65	0.62
I_2–DMSO	−2.13	4.23	−4.68	0.71	−7.12	0.64	−6.48	0.65
I_2–Me_3PO	−2.55	4.43	−4.99	0.70	−7.47	0.64	−6.83	0.64
I_2–Et_3N	−4.02	7.32	−4.99	0.98	−9.41	0.93	−8.32	0.92
I_2–quinuclidine	−6.02	7.30	−8.40	1.08	−12.15	1.03	−11.22	1.03
	B97-2		PBE1PBE		ωB97		B2PLYP	
complex	ΔE	BSSE	ΔE	BSSE	ΔE	BSSE	ΔE	BSSE
C_6F_5I–Et_3N	−2.22	0.78	−4.44	0.77	−7.70	0.69	−1.39	1.78
C_6F_5I–DMSO	−2.74	0.46	−4.17	0.47	−6.35	0.46	−2.73	1.00
C_4F_9I–Et_3N	−2.53	0.69	−4.71	0.67	−8.18	0.63	−1.86	1.63
C_4F_9I–DMSO	−2.92	0.44	−4.34	0.44	−6.82	0.40	−3.07	0.95
C_6F_5I–Me_3PO	−3.68	0.47	−4.94	0.47	−7.16	0.44	−3.43	1.00
C_4F_9I–Me_3PO	−3.94	0.46	−5.20	0.44	−7.73	0.39	−3.90	0.95
C_6F_5I–quinuclidine	−5.13	0.69	−6.62	0.69	−8.53	0.69	−3.81	1.68
C_4F_9I–quinuclidine	−3.98	0.63	−5.56	0.62	−8.04	0.59	−3.02	1.53
I_2–DMSO	−5.59	0.70	−7.40	0.65	−7.83	0.48	−4.64	1.88
I_2–Me_3PO	−6.26	0.69	−7.89	0.63	−8.59	0.45	−5.11	1.93
I_2–Et_3N	−7.56	1.02	−10.48	0.96	−9.99	0.68	−6.04	3.08
I_2–quinuclidine	−10.92	1.10	−12.94	1.05	−11.73	0.75	−9.00	3.14

[a]The calculated electronic energies of interaction, corrected for zero-point energy differences and BSSE are listed for each level of theory, along with the BSSE as estimated by the counterpoise method. See the Computational Methodology section for details.

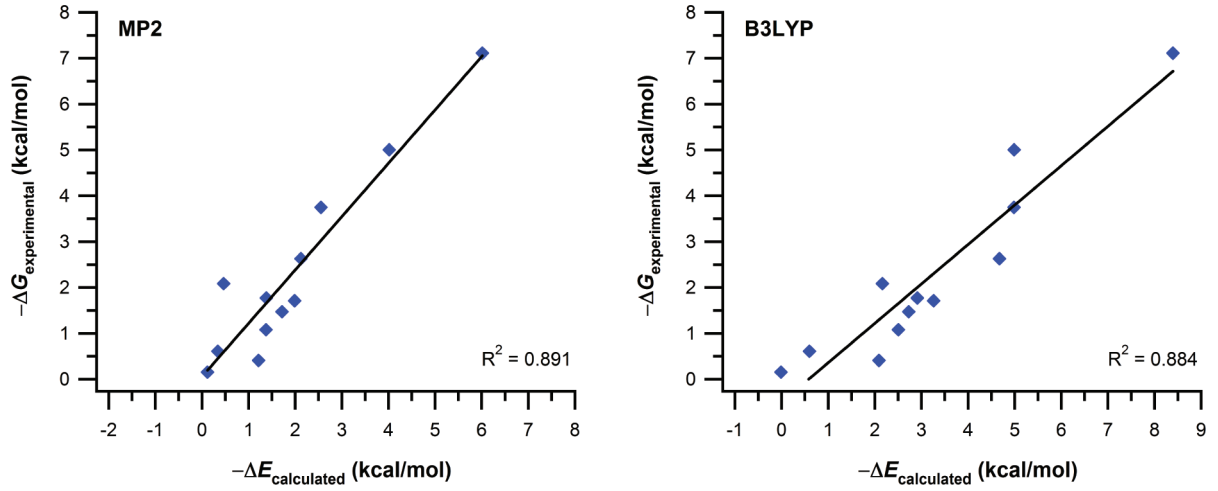

Figure 5. Plots of free energy of binding ($-\Delta G_{expt}$, from Table 1) versus calculated energy of interaction for model complexes ($-\Delta E_{calcd}$, from Table 3) at the MP2 and B3LYP levels of theory.

the context of noncovalent interactions.[49a,55] It is noteworthy that these functionals also provide superior performance to the *ab initio* MP2 method (R^2 = 0.89, Q^2 = 0.86), which has been applied extensively in computational studies of XB: the RMSE of 0.65 kcal/mol for the latter indicates the errors are more than twice those of the B97-1 functional. Members of the M0X family of meta-GGA functionals developed by Truhlar and co-workers, and recommended for broad applicability to chemical systems including noncovalent interactions, display relatively poor correlations with the experimental XB thermodynamic data. Likewise, the DFT-D dispersion-corrected methods tested here do not appear to provide an advantage, a somewhat surprising result given that dispersion forces almost certainly play a role in XB interactions of this type. It is important to note that the poor performance of these methods is not due to family-dependent behavior of the halogen bond donors, a

dx.doi.org/10.1021/jo300279m | J. Org. Chem. 2012, 77, 3483−3491

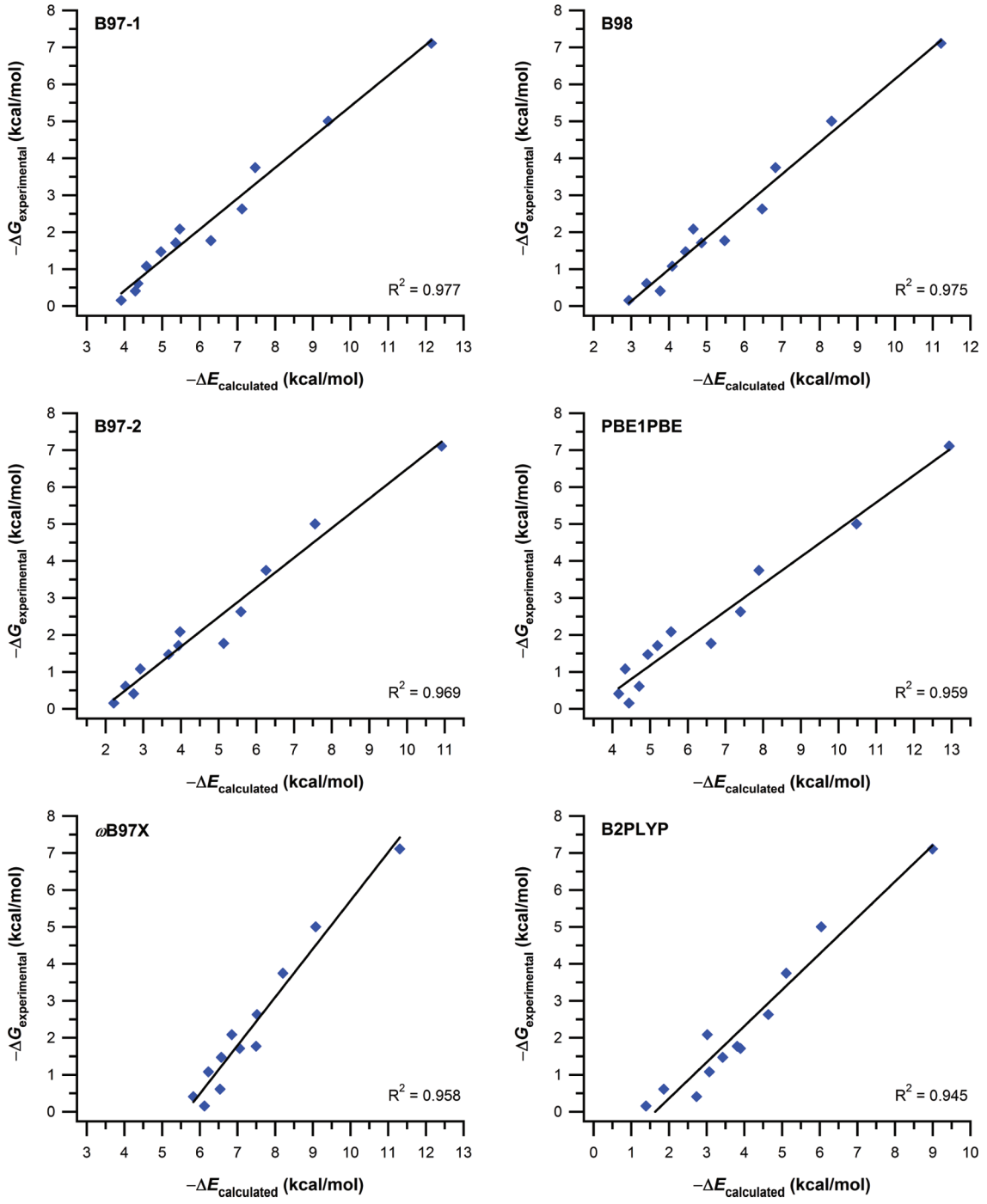

Figure 6. Plots of free energy of binding ($-\Delta G_{exptl}$, from Table 1) versus calculated energy of interaction for model complexes ($-\Delta E_{calcd}$, from Table 3) with the top six performing DFT functionals.

possibility that was assessed by separate analysis of the data for each of the iodo compounds studied.

The excellent performance of the top ranked functionals is consistent with previously reported results. Benchmarking studies by Zhao and Truhlar investigating the ability of various DFT functionals to model hydrogen bonding,[33,49a,b,d] dipole−dipole,[33,49a,b] van der Waals,[33,49a−d] $\pi-\pi$ stacking,[33,49b] and noncovalent interactions in general[33,49a,b] have consistently placed B97-1 in the top performing functionals, with B98 and PBE1PBE close to follow. Interestingly, B97-1 performed poorly in modeling charge-transfer interactions in these studies. Other benchmarking studies[55] have demonstrated that B97-1 performs well in modeling van der Waals interactions containing a significant charge-transfer component. Some of the top performing functionals in this study have been shown to provide the smallest deviations in energy from higher-level calculations in modeling halogen bonds of small halocarbon molecules with neutral Lewis bases (B97-1, B98, PBE1PBE)[49e] as well as halide−protein complexes (B97-1, B98).[56]

The correlations listed in Table 4 refer to single-point energy DFT calculations using geometries optimized at the MP2 level of theory. In light of the utility of the B97-1 functional in correlations with the experimental thermodynamic data, a second set of geometry optimizations of the complexes listed in Table 2

dx.doi.org/10.1021/jo300279m | J. Org. Chem. 2012, 77, 3483−3491

Table 4. Statistical Analysis Performed on Linear Regression Relationships between Calculated Gas-Phase Energies of Model Compounds and Experimental Solution-Phase Energies in Alkane Solvent from Table 1[a]

method	R^2	RSS	RMSE	Q^2	PRESS	RMSPE
B97-1	0.977	1.09	0.301	0.970	1.39	0.340
B98	0.975	1.15	0.310	0.968	1.50	0.353
B97-2	0.969	1.42	0.344	0.959	1.89	0.397
PBE1PBE	0.959	1.89	0.397	0.947	2.46	0.453
ωB97X	0.958	1.96	0.404	0.929	3.30	0.525
B2PLYP	0.945	2.55	0.461	0.926	3.43	0.534
MPW2PLYP	0.940	2.78	0.481	0.919	3.75	0.559
MPW2PLYP-D	0.920	3.73	0.558	0.899	4.71	0.626
X3LYP	0.897	4.81	0.633	0.851	6.92	0.760
MP2	0.891	5.09	0.651	0.857	6.66	0.745
ωB97X-D	0.888	5.20	0.658	0.860	6.51	0.737
B3LYP	0.884	5.41	0.672	0.830	7.91	0.812
HCTH	0.878	5.66	0.687	0.836	7.64	0.798
M05-2X	0.872	5.95	0.704	0.825	8.12	0.823
B2PLYP-D	0.848	7.05	0.766	0.792	9.65	0.897
M06	0.844	7.26	0.778	0.761	11.12	0.963
M06-HF	0.820	8.36	0.834	0.746	11.82	0.992
ωB97	0.817	8.51	0.842	0.763	11.00	0.958
M06-2X	0.810	8.84	0.858	0.736	12.27	1.011
M06-L	0.646	16.47	1.172	0.461	25.06	1.445
B97-D	0.607	18.29	1.235	0.410	27.44	1.512
M05	0.468	24.73	1.436	0.150	39.56	1.816
HF	0.00009	46.51	1.969	−0.544	71.82	2.447

[a]The statistical terms are defined as follows: R^2, the coefficient of determination between ΔG_{exptl} (Table 1) and ΔE (Table 3) for the entire data set; RSS, the residual sum of squares between free energies as predicted by the linear regression model and experimental free energies; RMSE, the root-mean-square error between free energies as predicted by the linear regression model and experimental free energies; Q^2, the cross-validated coefficient of determination as determined by the leave-one-out-method; PRESS, the corresponding predictive residual sum of squares for the cross-validation; RMSPE, the corresponding root-mean-square prediction error for the cross-validation. See the Supporting Information for details.

was carried out using this functional. For two of the 12 complexes (C_4F_9I–Et_3N and C_4F_9I–quinuclidine), convergence problems were encountered at the B97-1/6-31+G(d,p)-LANL2DZdp level of theory. However, for the remaining 10 complexes, the calculated gas-phase adiabatic energies of interaction determined using the B97-1 geometries also showed excellent correlation with the experimental data (R^2 = 0.979; Figure 7). For the latter set of data, scaled (0.9859)[29] DFT/B97-1 frequencies were employed for the zero-point energy corrections. The results indicate that, for the set of complexes studied here, an approach relying on the B97-1 DFT functional for both geometries and energies provides useful quantitative modeling of the thermodynamics of halogen bonding.

Correlations with Thermodynamic Data in Carbon Tetrachloride Solvent. To probe the generality of the conclusions reached on the basis of the data in alkane solvent, a second data set consisting of halogen bonding free energies in carbon tetrachloride (CCl_4) was analyzed. It encompasses interactions of a range of inorganic and organic donors: iodine (I_2), iodine monochloride (ICl), iodine monobromide (IBr), cyanogen iodide (ICN) and perfluorohexyl iodide ($C_6F_{13}I$), several of which were not included in the data from alkane solvent described above. In addition to the four Lewis bases listed above (quinuclidine, Et_3N, Bu_3PO and Bu_2SO), pyridine was also included, for a total of ten halogen-bonded complexes (Table 5). Although empirical metrics of solvent polarity, polarizability and cohesive energy reveal significant differences between alkanes and carbon tetrachloride,[57] including the ability of the latter to participate as a weak donor of halogen bonds, CCl_4 is generally considered to be a relatively inert solvent from

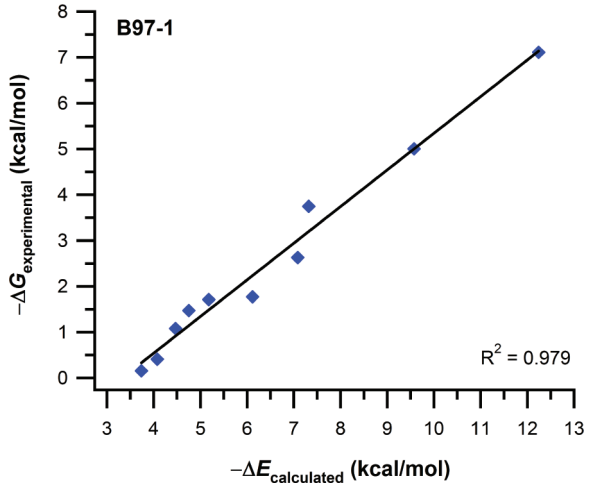

Figure 7. Plot of free energy of binding ($-\Delta G_{exptl}$, from Table 1) versus calculated (B97-1/6-31+G(d,p)-LANL2DZdp) energy of interaction for model complexes ($-\Delta E_{calcd}$), using geometries optimized at the B97-1/6-31+G(d,p)-LANL2DZdp level of theory (see the Supporting Information for details).

the perspective of noncovalent interactions. Correlations between the experimental data in CCl_4 from Table 5 and calculated energies of model complexes were examined, using the top seven performing methods as identified in the previous section as well as the MP2 method. As described above, C_4F_9I was used in place of $C_6F_{13}I$, Me_3PO in place of Bu_3PO and Me_2SO in place of Bu_2SO to expedite these calculations; geometries were optimized at the MP2 level of theory, followed by single-point

dx.doi.org/10.1021/jo300279m | J. Org. Chem. 2012, 77, 3483–3491

Table 5. Association Constants (K_a) and Free Energies of Interaction (ΔG_{exptl}) for Halogen-Bonded Complexes in Carbon Tetrachloride (CCl_4) Solvent

complex	K_a[a] (M^{-1})	ΔG_{exptl}[b] (kcal/mol)
$C_6F_{13}I$–Et_3N[c]	2.0 ± 0.4	−0.4 ± 0.1
$C_6F_{13}I$–Bu_3PO[c]	4.0 ± 0.8	−0.8 ± 0.1
$C_6F_{13}I$–quinuclidine[c]	16 ± 3.2	−1.6 ± 0.1
I_2–Bu_2SO[d]	24 ± 4.7	−1.9 ± 0.1
ICN–pyridine[e]	45 ± 9	−2.3 ± 0.1
I_2–pyridine[f]	78 ± 16	−2.6 ± 0.1
I_2–Bu_3PO[d]	111 ± 22	−2.8 ± 0.1
IBr–pyridine[f]	12300 ± 2500	−5.7 ± 0.1
ICl–pyridine[f]	229000 ± 46000	−7.4 ± 0.1

[a]Association constant (K_a) for the halogen-bonding interaction, determined by fitting changes in ^{19}F NMR chemical shift or charge-transfer band as a function of Lewis base concentration to a 1:1 binding isotherm. [b]Free energy of interaction calculated from K_a. [c]Data from ref 15. [d]Data from ref 61a. [e]Data from ref 61b. [f]Data from ref 61c.

Table 6. Statistical Analysis Performed on Linear Regression Relationships between Calculated Gas-Phase Energies of Model Complexes and Experimental Solution Phase Energies in Carbon Tetrachloride (CCl_4) Solvent from Table 5[a]

method	R^2	RSS	RMSE	Q^2	PRESS	RMSPE
B97-1	0.971	1.22	0.369	0.956	1.85	0.453
PBE1PBE	0.970	1.25	0.372	0.951	2.04	0.476
B98	0.961	1.64	0.427	0.937	2.65	0.543
B97-2	0.955	1.87	0.456	0.918	3.43	0.618
ωB97X	0.946	2.27	0.503	0.909	3.82	0.652
B2PLYP	0.946	2.28	0.503	0.906	3.94	0.662
MPW2PLYP	0.945	2.29	0.504	0.909	3.81	0.651
MP2	0.899	4.23	0.686	0.834	6.93	0.878

[a]The statistical terms are defined as in Table 4.

energy calculations using the seven listed DFT functionals (Table 6). A near equivalent level and order of performance for the various levels of theory was obtained. This result provides a strong indication that the identified DFT functionals are robust in their ability to model the thermodynamics of diverse XB interactions in nonpolar, noncompetitive solvents.[58] Given the widespread application of DFT for probing mechanisms and selectivities of organic reactions[59] and for studying drug–biomolecule interactions,[60] correlations of the type studied here may be valuable in instances where XB is proposed to play a role.

CONCLUSIONS

This investigation has employed experimental thermodynamic data for interactions between iodinated donors and neutral Lewis bases in noncompetitive solvents as the basis for a systematic evaluation of computational models of halogen bonding. The chosen data set is noteworthy for its inclusion of both inorganic (I_2) and organic (iodoperfluoroarene and -alkane) donors and spans roughly 7 kcal/mol in terms of the free energies of XB; it encompasses association constants at the lower limit of measurement in the solution phase, as well as some of the highest known for XB between neutral compounds in solution. Geometries optimized at the MP2/6-31+G(d,p)-LANL2DZdp level of theory were employed as the basis for single-point energy calculations at 23 levels of theory, including diverse DFT functionals. Relationships between calculated adiabatic energies of interaction and experimental thermodynamic data from alkane solvents were analyzed. A variety of metrics, including those based on cross-validation by the leave-one-out statistical method, indicate that certain DFT functionals, in particular, the related GGA functionals B97-1, B97-2, and B98, provide very good levels of correlation with the experimental data. The results of correlations with a second set of experimental thermodynamic data, differing from the first in the identity of both the halogen bond donors and the solvent, were in excellent quantatitive agreement with these conclusions.

ASSOCIATED CONTENT

Supporting Information

Complete data sets, graphs, details of statistical analysis and coordinates of calculated structures. This material is available free of charge via the Internet at http://pubs.acs.org.

AUTHOR INFORMATION

Corresponding Author

*E-mail: mtaylor@chem.utoronto.ca.

Notes

The authors declare no competing financial interest.

ACKNOWLEDGMENTS

This work was supported by NSERC (Discovery Grants Program, Graduate Fellowship to M.G.C.), the Canadian Foundation for Innovation, and the Ontario Ministry of Research and Innovation.

REFERENCES

(1) Legon, A. C. *Phys. Chem. Chem. Phys.* **2010**, *12*, 7736–7747.
(2) (a) Benesi, H. A.; Hildebrand, J. H. A *J. Am. Chem. Soc.* **1949**, *71*, 2703–2707. (b) Hassel, O. *Science* **1970**, *170*, 497–502. (c) Laurence, C.; Queignec-Cabanetos, M.; Dziembowska, T.; Queignec, R.; Wojtkowiak, B. *J. Am. Chem. Soc.* **1981**, *103*, 2567–2573.
(3) Metrangolo, P.; Meyer, F.; Pilati, T.; Resnati, G.; Terraneo, G. *Angew. Chem., Int. Ed.* **2008**, *47*, 6114–6127.
(4) (a) Sarwar, M. G.; Dragisic, B.; Sagoo, S.; Taylor, M. S. *Angew. Chem., Int. Ed.* **2010**, *49*, 1674–1677. (b) Kilah, N. L.; Wise, M. D.; Serpell, C. J.; Thompson, A. L.; White, N. G.; Christensen, K. E.; Beer, P. D. *J. Am. Chem. Soc.* **2010**, *132*, 11893–11895. (c) Caballero, A.; White, N. G.; Beer, P. D. *Angew. Chem. Int.* **2011**, *50*, 1845–1848. (d) Chudzinski, M. G.; McClary, C. A.; Taylor, M. S. *J. Am. Chem. Soc.* **2011**, *133*, 10559–10567.
(5) (a) Auffinger, P.; Hays, F. A.; Westhof, E.; Ho, P. S. *Proc. Natl. Acad. Sci. U.S.A.* **2004**, *101*, 16789–16794. (b) Hardegger, L. A.; Kuhn, B.; Spinnler, B.; Anselm, L.; Ecabert, R.; Stihle, M.; Gsell, B.; Thoma, R.; Diez, J.; Benz, J.; Plancher, J.-M.; Hartmann, G.; Banner, D. W.; Haap, W.; Diederich, F. *Angew. Chem., Int. Ed.* **2011**, *50*, 314–318.
(6) Mulliken, R. S. *J. Am. Chem. Soc.* **1950**, *72*, 600–608.
(7) Politzer, P.; Lane, P.; Concha, M. C.; Ma, Y.; Murray, J. S. *J. Mol. Model.* **2007**, *13*, 305–311.
(8) (a) Lommerse, J. P. M; Stone, A. J.; Taylor, R.; Allen, F. H. *J. Am. Chem. Soc.* **1996**, *118*, 3108–3116. (b) Zou, J.-W.; Jiang, Y.-J.; Guo, M.; Hu, G.-X.; Zhang, B.; Liu, H.-C.; Yu, Q.-S. *Chem.—Eur. J.* **2005**, *11*, 740–751. (c) Lu, Y.-X.; Zou, J.-W.; Wang, Y.-H.; Yu, Q.-S. *J. Mol Struct. THEOCHEM* **2006**, *776*, 83–87. (d) Lu, Y.-X.; Zou, J.-W.; Wang, Y.-H.; Jiang, Y.-J.; Yu, Q.-S. *J. Phys. Chem. A* **2007**, *111*, 10781–10788. (e) Riley, K. E.; Murray, J. S.; Politzer, P.; Concha, M. C.; Hobza, P. *J. Chem. Theory Comput.* **2009**, *5*, 155–163.
(9) Riley, K. E.; Hobza, P. *J. Chem. Theory Comput.* **2008**, *4*, 232–242.
(10) (a) Alkorta, I.; Rozas, I.; Elguero, J. *J. Phys. Chem. A* **1998**, *102*, 9278–9285. (b) Karpfen, A. *J. Phys. Chem. A* **2000**, *104*, 6871–6879. (c) Wang, W.; Wong, N.-B.; Zheng, W.; Tian, A. *J. Phys. Chem. A*

2004, *108*, 1799−1805. (d) Riley, K. E.; Merz, K. M. Jr. *J. Phys. Chem. A* **2007**, *111*, 1688−1694.
(11) (a) Lamarche, O.; Platts, J. A. *Chem.—Eur. J.* **2002**, *8*, 457−466. (b) Bessau, F.; Graton, J.; Berthelot, M. *Chem.—Eur. J.* **2008**, *14*, 10656−10669. (c) Nocker, M.; Handschuh, S.; Tautermann, C.; Liedl, K. R. *J. Chem. Inf. Model.* **2009**, *49*, 2067−2076.
(12) (a) Karpfen, A. *Struct. Bonding (Berlin)* **2008**, *126*, 1−15. (b) Davey, J. B.; Legon, A. C.; Thumwood, J. M. A. *J. Chem. Phys.* **2001**, *114*, 6190−6202.
(13) Bianchi, R.; Forni, A.; Pilati, T. *Chem.—Eur. J.* **2003**, *9*, 1631−1638.
(14) (a) Rege, P. D.; Malkina, O. L.; Goroff, N. S. *J. Am. Chem. Soc.* **2002**, *124*, 370−371. (b) Glaser, R.; Chen, N.; Wu, H.; Knotts, N.; Kaupp, M. *J. Am. Chem. Soc.* **2004**, *126*, 4412−4419.
(15) Laurence, C.; Graton, J.; Berthelot, M.; El Ghomari, M. J. *Chem.—Eur. J.* **2011**, *17*, 10431−10444.
(16) Cabot, R.; Hunter, C. A. *Chem. Commun.* **2009**, 2005−2007.
(17) Dimitrijević, E.; Kvak, O.; Taylor, M. S. *Chem. Commun.* **2010**, *46*, 9025−9027.
(18) (a) Sarwar, M. G.; Dragisic, B.; Salsberg, L. J.; Gouliaras, C.; Taylor, M. S. *J. Am. Chem. Soc.* **2010**, *132*, 1646−1653. (b) Lu, Y.; Li, H.; Zhu, X.; Zhu, W.; Liu, H. *J. Phys. Chem. A* **2011**, *115*, 4467−4475.
(19) (a) Zhao, Y.; Truhlar, D. G. *Acc. Chem. Res.* **2008**, *41*, 157−167. (b) Zhao, Y.; Truhlar, D. G. *J. Chem. Theory Comput.* **2008**, *4*, 1849−1868.
(20) (a) Veitch, G. E.; Jacobsen, E. N. *Angew. Chem., Int. Ed.* **2010**, *49*, 7332−7335. (b) Walter, S. M.; Kniep, F.; Herdtweck, E.; Huber, S. M. *Angew. Chem., Int. Ed.* **2011**, *50*, 7187−7191. (c) Guilbault, A.-A.; Legault, C. Y. *ACS Catal.* **2012**, *2*, 219−222.
(21) Frisch, M. J.; Trucks, G. W.; Schlegel, H. B.; Scuseria, G. E.; Robb, M. A.; Cheeseman, J. R.; Scalmani, G.; Barone, V.; Mennucci, B.; Petersson, G. A.; Nakatsuji, H.; Caricato, M.; Li, X.; Hratchian, H. P.; Izmaylov, A. F.; Bloino, J.; Zheng, G.; Sonnenberg, J. L.; Hada, M.; Ehara, M.; Toyota, K.; Fukuda, R.; Hasegawa, J.; Ishida, M.; Nakajima, T.; Honda, Y.; Kitao, O.; Nakai, H.; Vreven, T.; Montgomery, Jr., J. A.; Peralta, J. E.; Ogliaro, F.; Bearpark, M.; Heyd, J. J.; Brothers, E.; Kudin, K. N.; Staroverov, V. N.; Kobayashi, R.; Normand, J.; Raghavachari, K.; Rendell, A.; Burant, J. C.; Iyengar, S. S.; Tomasi, J.; Cossi, M.; Rega, N.; Millam, N. J.; Klene, M.; Knox, J. E.; Cross, J. B.; Bakken, V.; Adamo, C.; Jaramillo, J.; Gomperts, R.; Stratmann, R. E.; Yazyev, O.; Austin, A. J.; Cammi, R.; Pomelli, C.; Ochterski, J. W.; Martin, R. L.; Morokuma, K.; Zakrzewski, V. G.; Voth, G. A.; Salvador, P.; Dannenberg, J. J.; Dapprich, S.; Daniels, A. D.; Farkas, Ö.; Foresman, J. B.; Ortiz, J. V.; Cioslowski, J.; Fox, D. J. *Gaussian 09, Revision B.01*; Gaussian, Inc.: Wallingford, CT, 2009.
(22) (a) Møller, C.; Plesset, M. S. *Phys. Rev.* **1934**, *46*, 618−622. (b) Head-Gordon, M.; Pople, J. A.; Frisch, M. J. *Chem. Phys. Lett.* **1988**, *153*, 503−506.
(23) Hehre, W. J.; Radom, L.; Schleyer, P. v. R.; Pople, J. A. *Ab Initio Molecular Orbital Theory*; Wiley: New York, 1986.
(24) Hay, J. P.; Wadt, W. R. *J. Chem. Phys.* **1985**, *82*, 270−283.
(25) Check, C. E.; Faust, T. O.; Bailey, J. M.; Wright, B. J.; Gilbert, T. M.; Sunderlin, L. S. *J. Phys. Chem. A* **2001**, *105*, 8111−8116.
(26) https://bse.pnl.gov/bse/portal. Schuchardt, K. L.; Didier, B. T.; Eisethagen, T.; Sun, L.; Gurumoorthi, V.; Chase, J.; Li, J.; Windus, T. L. *J. Chem. Inf. Model.* **2007**, *47*, 1045−1052.
(27) Tight convergence criteria were applied to quinuclidine, C_6F_5I, and C_4F_9I−Et_3N. Geometry optimization of representative complexes under normal or tight convergence criteria that had no imaginary frequencies in both cases resulted in energy differences $<10^{-7}$ hartrees. Conformational analysis performed on complexes of DMSO with the halogen bond donors confirmed global minima were obtained.
(28) Boys, S. F.; Bernardi, F. *Mol. Phys.* **1970**, 553−566.
(29) Merrick, J. P.; Moran, D.; Radom, L. *J. Phys. Chem. A* **2007**, *111*, 11683−11700.
(30) Becke, A. D. *J. Chem. Phys.* **1993**, *98*, 5648−5652.
(31) (a) Lee, C.; Yang, W.; Parr, R. G. *Phys. Rev. B* **1988**, *37*, 785−789. (b) Miehlich, B.; Savin, A.; Stoll, H.; Preuss, H. *Chem. Phys. Lett.* **1989**, *157*, 200−206.
(32) Zhao, Y.; Schultz, N. E.; Truhlar, D G. *J. Chem. Phys.* **2005**, *123*, 161103.
(33) Zhao, Y.; Truhlar, D. G. *J. Chem. Theory Comput.* **2006**, *2*, 364−382.
(34) Zhao, Y.; Truhlar, D. G. *Theor. Chem. Acc.* **2008**, *120*, 215−241.
(35) Zhao, Y.; Truhlar, D. G. *J. Phys. Chem. A* **2006**, *110*, 13126−13130.
(36) Zhao, Y.; Truhlar, D. G. *J. Chem. Phys.* **2006**, *125*, 194101.
(37) Chai, J.-D.; Head-Gordon, M. *J. Chem. Phys.* **2008**, *128*, 084106.
(38) Chai, J.-D.; Head-Gordon, M. *Phys. Chem. Chem. Phys.* **2008**, *10*, 6615−6620.
(39) Xu, X.; Goddard, W. A. III *Proc. Natl. Acad. Sci. U.S.A.* **2004**, *101*, 2673−2677.
(40) (a) Perdew, J. P.; Burke, K.; Ernzerhof, M. *Phys. Rev. Lett.* **1996**, *77*, 3865−3868. (b) Adamo, C.; Barone, V. *J. Chem. Phys.* **1999**, *110*, 6158−6169.
(41) Boese, A. D.; Handy, N. C. *J. Chem. Phys.* **2001**, *114*, 5497−5503.
(42) Hamprecht, F. A.; Cohen, A.; Tozer, D. J.; Handy, N. C. *J. Chem. Phys.* **1998**, *109*, 6264−6271.
(43) Wilson, P. J.; Bradley, T. J.; Tozer, D. J. *J. Chem. Phys.* **2001**, *115*, 9233−9242.
(44) Schmider, H. L.; Becke, A. D. *J. Chem. Phys.* **1998**, *108*, 9624−9631.
(45) Grimme, S. *J. Comput. Chem.* **2006**, *27*, 1787−1799.
(46) Grimme, S. *J. Chem. Phys.* **2006**, *124*, 034108.
(47) Schwabe, T.; Grimme, S. *Phys. Chem. Chem. Phys.* **2007**, *9*, 3397.
(48) Schwabe, T.; Grimme, S. *Phys. Chem. Chem. Phys.* **2006**, *8*, 4398−4401.
(49) (a) Zhao, Y.; Truhlar, D. G. *J. Chem. Theory Comput.* **2005**, *1*, 415−432. (b) Zhao, Y.; Truhlar, D. G. *J. Phys. Chem. A* **2005**, *109*, 5656−5667. (c) Zhao, Y.; Truhlar, D. G. *J. Phys. Chem. A* **2006**, *110*, 5121−5129. (d) Zhao, Y.; Truhlar, D. G. *J. Phys. Chem. A* **2004**, *108*, 6908−6918. (e) Lu, Y.-X.; Zou, J.-W.; Fan, J.-C.; Zhao, W.-N.; Jiang, Y.-J.; Yu, Q.-S. *J. Comput. Chem.* **2009**, *30*, 725−732. (f) Burns, L. A.; Vázquez-Mayagoitia, Á.; Sumpter, B. G.; Sherrill, C. D. *J. Chem. Phys.* **2011**, *134*, 084107.
(50) Bondi, A. *J. Phys. Chem.* **1964**, *68*, 441−451.
(51) Hunter, C. A. *Angew. Chem., Int. Ed.* **2004**, *53*, 5310−5324.
(52) Cook, J. L.; Hunter, C. A.; Low, C. M. R.; Perez-Velasco, A.; Vinter, J. G. *Angew. Chem., Int. Ed.* **2007**, *46*, 3706−3709.
(53) Cabot, R.; Hunter, C. A.; Varley, L. M. *Org. Biomol. Chem.* **2010**, *8*, 1455−1462.
(54) To test whether this problem arises from limitations of the AM1 electrostatic potential calculations, similar calculations were carried out at higher levels of theory (B3LYP/6-31+G(d,p)-LANL2DZdp and MP2/6-31+G(d,p)-LANL2DZdp). The same hierarchy of donor abilities ($\alpha_{C6F5I} > \alpha_{C8F17I} > \alpha_{I2}$) was obtained regardless of the level of theory employed.
(55) Johnson, E. R.; DiLabio, G. A. *Chem. Phys. Lett.* **2006**, *419*, 333−339.
(56) Liu, X.; Zhou, P.; Shang, Z. *J. Mol. Model.* **2011**, in press. DOI: 10.1007/s00894-011-1232-z.
(57) (a) Reichardt, C. *Solvent and Solvent Effects in Organic Chemistry*, 3rd ed.; Wiley-VCH: Weinheim, Germany, 2003. (b) Cabot, R.; Hunter, C. A.; Varley, L. M. *Org. Biomol. Chem.* **2010**, *8*, 1455−1462.
(58) We note that attempts to extend these models to the Br_2−pyridine complex (for which the association constant is known in CCl_4) were unsuccessful, suggesting that these particular correlations may be restricted to iodine-based donors.
(59) Cheong, P. H.-Y.; Legault, C. Y.; Um, J. M.; Çelebi-Ölçüm, N.; Houk, K. N. *Chem. Rev.* **2011**, *111*, 5042−5137.
(60) LaPointe, S. M.; Weaver, D. F. *Curr. Comput.-Aided Drug Des.* **2007**, *3* (4), 290−296.
(61) (a) Laurence, C.; Gal, J.-F. *Lewis Basicity and Affinity Scales: Data and Measurement*; John Wiley & Sons: Chichester, U.K., 2010. (b) De Leeuw, J.; Van Cauteren, M.; Zeegers-Huyskens, T. *Spectrosc. Lett.* **1974**, *7*, 607−614. (c) Aloisi, G.; Beggiato, G. G.; Mazzucato, U. *Trans. Faraday Soc.* **1970**, *66*, 3075−3080.